

Supporting information for

Trigonal bipyramidal 5d-4f molecules with SMM behavior

Mohamed R. Saber, and Kim R. Dunbar

Department of Chemistry, Texas A&M University, College Station, Texas 77842-3012

RECEIVED DATE (automatically inserted by publisher); E-mail: dunbar@mail.chem.tamu.edu

Contents:

Experimental Section

Table S 1. Crystal structural data and refinement parameters for compounds 1–3.....	4
Table S 2 Selected bond distances (Å) and bond angles (°) for 1.....	5
Table S 3. Selected bond distances (Å) and bond angles (°) for 2.....	6
Table S 4. Selected bond distances (Å) and bond angles (°) for 3.....	7
Table S 5. Infrared spectral data for compounds 1–3 (cm ⁻¹).....	8
S 1. Distorted hexadecahedral polyhedron of La ³⁺ center in 1 (top). Asymmetric unit of 1. Thermal ellipsoids drawn at 30% probability. Hydrogen atoms omitted for clarity.....	9
S 2. Asymmetric unit of 2. Thermal ellipsoids drawn at 30% probability. Hydrogen atoms omitted for clarity.....	10
S 3. Asymmetric unit of 3. Thermal ellipsoids drawn at 30% probability. Hydrogen atoms omitted for clarity.....	11
S 4. (a) Temperature dependence of $\chi(\Diamond)$ and χT product (O) for 1 . Solid line corresponds to fit using PHI (S=1/2, g = 1.88 and TIP = 2.49×10^{-3}). (b) Reduced magnetization data at different external fields. Inset: field dependent magnetization. The solid line corresponds to the Brillouin function (S = 1/2, $g_{avg} = 1.78$) ..	12
S 5. (a) Temperature dependence of $\chi(\Diamond)$ and the χT product (O) for 2 . (b) reduced magnetization data at different external fields. Inset: field dependent magnetization for 2 (O).....	13
S 6. Temperature dependence of the out-of-phase AC susceptibility of 2 (top) and fit of the temperature dependence of the AC susceptibility data for 2 (bottom) under a zero applied DC field.....	14
S 7. Temperature dependence of the out-of-phase AC susceptibility of 2 (top) and fit of the temperature dependence of the AC susceptibility of 2 (bottom) under a 1000 Oe DC applied field.....	15
S 8. Field dependence AC data for 2	16
S 9. (a) Temperature dependence of $\chi(\Diamond)$ and the χT product (O) for 3 . (b) reduced magnetization data at different external fields. Inset: field dependent magnetization for 3 (O).....	17
S 10. Temperature dependence of the out-of-phase ac susceptibility of 3 (top), and fit of Temperature dependence of ac susceptibility of 3 (bottom) under a zero DC applied field.....	18
S 11. Temperature dependence of the out-of-phase AC susceptibility data of 3 (top) and fit of the temperature dependence of AC susceptibility of 3 (bottom) under a 1000Oe DC applied field.....	19
S 12. Field dependence AC data for 3	20

Experimental Section

Starting materials. All chemicals and solvents were of reagent grade quality. The synthesis of the precursor (Et_4N^+)[triphosRe(CN)₃] was performed according to the reported procedure.¹ All reactions were carried out under nitrogen using standard Schlenk-line techniques.

Physical Measurements. Elemental analyses were performed by Atlantic Microlab Inc. (Norcross, GA). Infrared spectra were recorded as Nujol mulls in the range 220–4000 cm⁻¹ on a Nicolet IR/42 spectrophotometer.

General synthesis of metal complexes:

Single crystals were obtained by mixing solutions of $\text{Ln}(\text{NO}_3)_3 \cdot 6\text{H}_2\text{O}$ {where Ln = La, Tb or Dy} (0.075 mmol) in 2 mL of CH₃CN with solutions of (Et_4N^+)[triphosRe(CN)₃] (50 mg, 0.049 mmol) in acetonitrile (3 mL). After standing overnight, the solutions produced orange-brown crystals of the products (Et_4N^+)₂[triphosRe(CN)₃)₂(Ln(NO₃)₃)₃]⁻·4CH₃CN {where Ln = La, Tb or Dy} which were harvested and washed with Et₂O.

(Et_4N^+)₂[triphosRe(CN)₃)₂(La(NO₃)₃)₃]⁻·4CH₃CN (1·4CH₃CN). (Yield = 62 mg, 83%). Elemental analysis: Calcd. for Re₂La₃C₁₀₄H₁₁₈N₁₇O₂₇P₆: C, 41.46; H, 3.95; N, 7.90; Found: C, 41.24; H, 4.06; N, 8.06%. IR (Nujol): ν (C≡N) 2072(m), 2090(m) cm⁻¹.

(Et_4N^+)₂[triphosRe(CN)₃)₂(Tb(NO₃)₃)₃]⁻·4CH₃CN (2·4CH₃CN). (Yield = 62 mg, 82%). Elemental analysis: Calcd. for Re₂Tb₃C₁₀₄H₁₁₈N₁₇O₂₇P₆: C, 40.65; H, 3.87; N, 7.75; Found: C, 40.38; H, 3.86; N, 7.78%. IR (Nujol): ν (C≡N) 2086(m), 2102(m) cm⁻¹.

(Et_4N^+)₂[triphosRe(CN)₃)₂(Dy(NO₃)₃)₃]⁻·4CH₃CN (3·4CH₃CN). (Yield = 64 mg, 84%). Elemental analysis: Calcd. for Re₂Dy₃C₁₀₄H₁₁₈N₁₇O₂₇P₆: C, 40.50; H, 3.86; N, 7.72; Found: C, 40.08; H, 3.86; N, 7.88%. IR (Nujol): ν (C≡N) 2086(m), 2103(m) cm⁻¹.

X-ray Crystallographic Measurements

X-ray single crystallographic data were collected on a Bruker-APEX CCD diffractometer at 110 K. The data sets were collected with Mo-K α radiation ($\lambda = 0.71073 \text{ \AA}$) as four ω -scans at a 0.3 – 0.4° step width. Data integration and processing, Lorentz-polarization and absorption corrections were performed using the Bruker SAINT² and SADABS³ software packages. Solution and refinement of the crystal structures was carried out using the SHELX⁴ suite of programs within the graphical interface X-SEED.⁵ The structures were solved by direct methods and refined by alternating cycles of full-matrix least-squares methods on F², using SHELXTL which resolved all non-hydrogen atoms which were refined anisotropically at the final refinement cycle. The hydrogen atoms were located from difference Fourier maps, assigned with isotropic displacement factors, and included in the final refinement cycles by use of geometrical constraints (HFIX for hydrogen atoms with parent carbon atoms. For 1, there was not enough electron density to assign Q peaks for one acetonitrile molecule but the equivalent void is clear in the crystal structure. A summary of the crystallographic data and unit cell parameters, conditions related to data collection and structural refinement statistics is provided in Table S1. Selected metal–ligand bond distances and angles are provided in Tables S2–S4.

Table S 1. Crystal structural data and refinement parameters for compounds **1–3**.

Compound	1	2	3
Space group	<i>C</i> 2/c	<i>C</i> 2/c	<i>C</i> 2/c
Unit cell	<i>a</i> = 36.170(7) Å <i>b</i> = 13.788(3) Å <i>c</i> = 26.153(5) Å β = 103.07(3) $^\circ$	<i>a</i> = 36.149(7) Å <i>b</i> = 13.737(3) Å <i>c</i> = 26.215(5) Å β = 103.85(3) $^\circ$	<i>a</i> = 36.167(7) Å <i>b</i> = 13.819(3) Å <i>c</i> = 26.339(5) Å β = 104.08(3) $^\circ$
Unit cell volume, <i>V</i>	12704.9 Å ³	12640(4) Å ³	12768(4) Å ³
<i>Z</i>	4	4	4
Density, ρ_{calc}	1.618 g/cm ³	1.701 g/cm ³	1.690 g/cm ³
Abs. coeff., μ	3.036 mm ⁻¹	3.719 mm ⁻¹	3.775 mm ⁻¹
Crystal color and habit	Orange Block	Orange Block	Orange Block
Crystal size	0.21 x 0.11 x 0.1 mm	0.25 x 0.18 x 0.12 mm	0.18 x 0.07 x 0.05 mm
Temperature	150 K	110 K	150 K
Radiation, λ	Mo-K α , 0.71073 Å	Mo-K α , 0.71073 Å	Mo-K α , 0.71073 Å
Min. and max. θ	1.16 to 27.46 $^\circ$	2.19 to 26.73 $^\circ$	1.58 to 26.02 $^\circ$
Reflections collected	69706 [$R_{\text{int}} = 0.0364$]	67419 [$R_{\text{int}} = 0.0311$]	63978 [$R_{\text{int}} = 0.0449$]
Independent reflections	14378	14557	14093
Data/parameters/restrains	14378/742/0	13403/778/3	12528/779 /3
R [$F_{\text{o}} > 4\sigma(F_{\text{o}})$]	$R_1 = 0.032$ $wR_2 = 0.0851$	$R_1 = 0.0504$ $wR_2 = 0.1301$	$R_1 = 0.052$ $wR_2 = 0.1308$
G.o.f. on F^2	1.065	1.073	1.065
Max./min. residual densities, e·Å ⁻³	0.33, -0.37	5.79, -2.6	1.23, -0.92

[a] $R_1 = \Sigma ||F_{\text{o}}| / |F_{\text{c}}|| \Sigma |F_{\text{o}}|$. [b] $wR_2 = [\sum [w(F_{\text{o}}^2 - F_{\text{c}}^2)^2] / \sum [w(F_{\text{o}}^2)^2]]^{1/2}$

Table S 2 Selected bond distances (\AA) and bond angles ($^\circ$) for **1**.

Compound 19	Distance (\AA)		Angle ($^\circ$)
La(1)-N(1)	2.567(4)	N(1)- La(1)-O(1)	77.4(1)
La (1) – N(3)	2.580(4)	N(1)- La(1)-O(2)	110.1(1)
La(1) – O(1)	2.732(3)	N(1)- La(1)-O(3)	71.6(1)
La(1) – O(2)	2.738(4)	N(1)- La(1)-O(4)	73.3(1)
La(1) – O(3)	2.600(5)	N(1)- La(1)-O(5)	143.2(1)
La(1) – O(4)	2.575(5)	N(1)- La(1)-O(6)	133.4(1)
La(1) – O(5)	2.567(3)	N(1)- La(1)-O(7)	69.6(1)
La(1) – O(6)	2.555(3)	N(1)- La(1)-O(8)	80.3(1)
La(1) – O(7)	2.8101(7)	N(1)- La(1)-N(3)	139.7(1)
La(1) – O(8)	2.606(4)	La(1)- N(1)-C(1)	159.7(4)
Re(1) – C(1)	2.071(4)	La(2)- N(2)-C(2)	158.7(3)
Re(1) – C(2)	2.059(4)	La(3)- N(3)-C(3)	157.8(3)
Re(1) – C(3)	2.077(4)	La(1)- O(1)-La(2)	166.2(1)
C(1) – N(1)	1.157(5)	Re(1)- C(1)-N(1)	171.1(4)
C(2) – N(2)	1.163(5)	Re(1)- C(2)-N(2)	173.0(4)
C(3) – N(3)	1.154(6)	Re(1)- C(3)-N(3)	170.9(4)
La(1) ... La(2)	5.399(1)		
La(2) ... La(3)	5.399(1)		
La(1) ... La(3)	5.609(1)		

Table S 3. Selected bond distances (\AA) and bond angles ($^\circ$) for **2**.

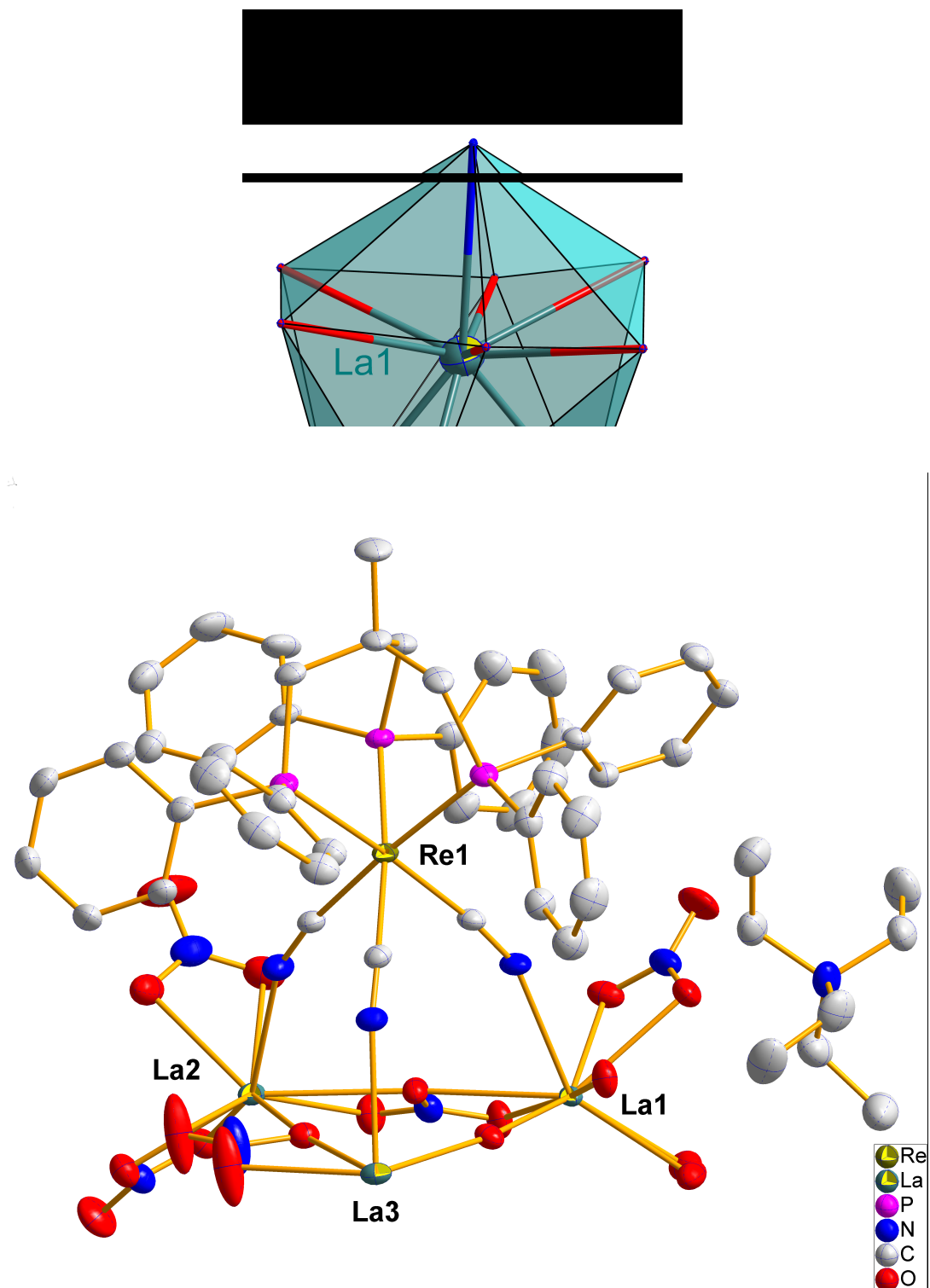
Compound 25	Distance (\AA)		Angle ($^\circ$)
Tb(1)-N(1)	2.408(7)	N(1)- Tb(1)-O(1)	77.2(2)
Tb(1)- N(3)	2.401(6)	N(1)- Tb(1)-O(2)	72.8(2)
Tb(1)- O(1)	2.606(5)	N(1)- Tb(1)-O(3)	139.6(2)
Tb(1)- O(2)	2.579(7)	N(1)- Tb(1)-O(4)	142.2(2)
Tb(1)- O(3)	2.523(8)	N(1)- Tb(1)-O(5)	75.2(2)
Tb(1)- O(4)	2.467(8)	N(1)- Tb(1)-O(6)	76.8(2)
Tb(1)- O(5)	2.449(5)	N(1)- Tb(1)-O(7)	81.9(2)
Tb(1)- O(6)	2.455(5)	N(1)- Tb(1)-O(8)	71.5(2)
Tb(1)- O(7)	2.507(6)	N(1)- Tb(1)-N(3)	139.9(2)
Tb(1)- O(8)	2.457(5)	Tb(1)- N(1)-C(1)	159.8(6)
Re(1)- C(1)	2.058(8)	Tb(2)- N(2)-C(2)	161.3(6)
C(1)- N(1)	1.15(1)	Tb(3)- N(3)-C(3)	159.8(6)
Tb(1) ... Tb(2)	5.160(1)	Tb(1)- O(1)-Tb(2)	168.0(2)
Tb(1) ... Tb(3)	5.521(1)	Re(1)- C(1)-N(1)	170.3(7)

Table S 4. Selected bond distances (\AA) and bond angles ($^\circ$) for **3**.

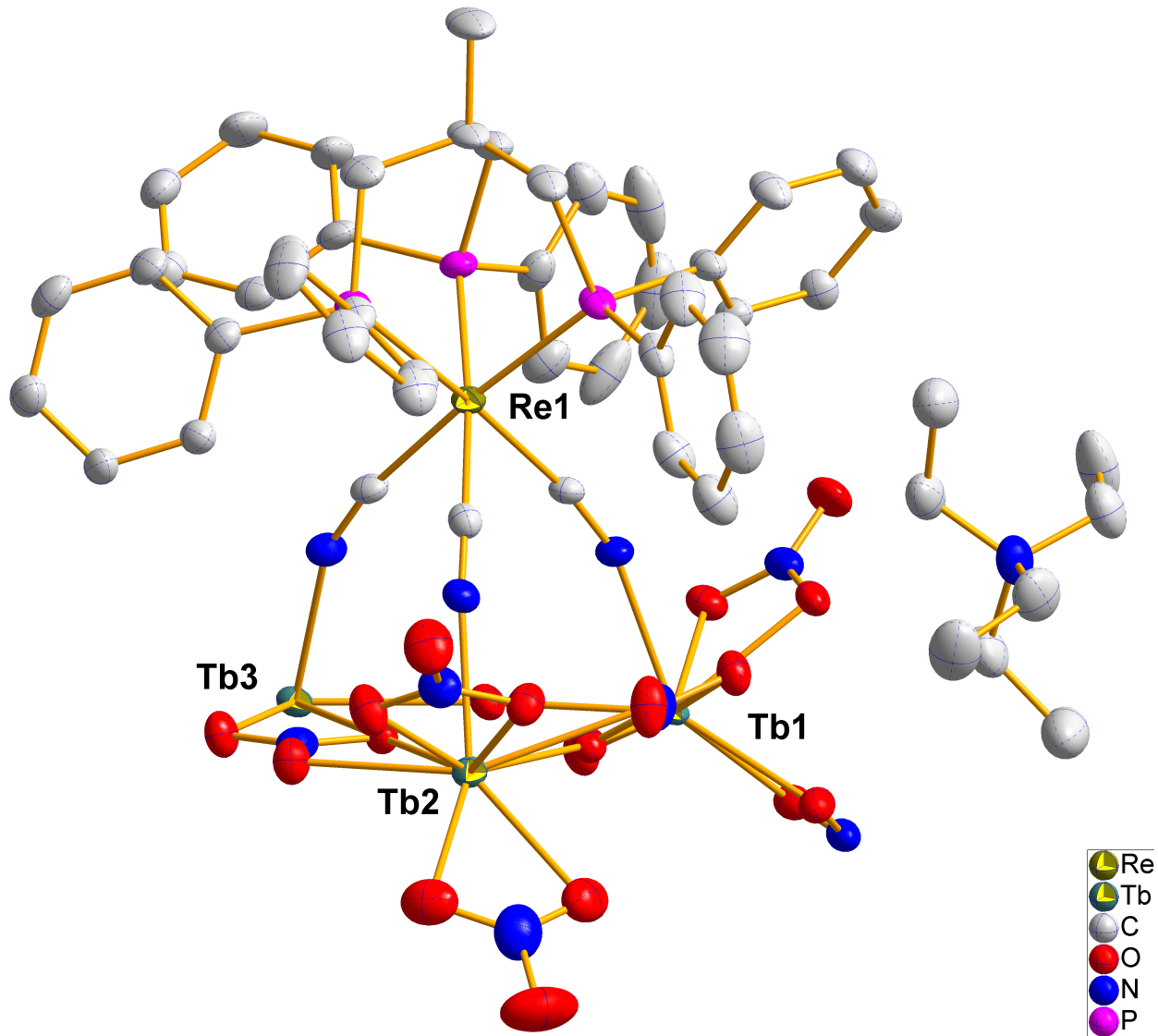
Compound 3	Distance (\AA)		Angle ($^\circ$)
Dy(1)-N(1)	2.388(7)	N(1)- Dy(1)-O(1)	76.8(2)
Dy(1) – N(3)	2.382(7)	N(1)- Dy(1)-O(2)	73.2(3)
Dy(1) – O(1)	2.626(6)	N(1)- Dy(1)-O(3)	71.1(2)
Dy(1) – O(2)	2.573(7)	N(1)- Dy(1)-O(4)	81.5(2)
Dy(1) – O(3)	2.7754(7)	N(1)- Dy(1)-O(5)	75.2(2)
Dy(1) – O(4)	2.499(7)	N(1)- Dy(1)-O(6)	77.5(2)
Dy(1) – O(5)	2.439(7)	N(1)- Dy(1)-O(7)	142.9(3)
Dy(1) – O(6)	2.443(7)	N(1)- Dy(1)-O(8)	149.7(3)
Dy(1) – O(7)	2.45(1)	N(1)- Dy(1)-N(3)	139.1(3)
Dy(1) – O(8)	2.43(1)	Dy(1)- N(1)-C(1)	160.2(7)
Re(1) – C(1)	2.074(8)	Dy(2)- N(2)-C(2)	162.5(6)
C(1) – N(1)	1.16(1)	Dy(3)- N(3)-C(3)	159.2(7)
Dy(1) ... Dy(2)	5.188(1)	Dy(1)- O(1)-Dy(2)	167.5(2)
Dy(1) ... Dy(3)	5.551(1)	Re(1)- C(1)-N(1)	169.7(7)

Table S 5. Infrared spectral data for compounds **1-3** (cm⁻¹)

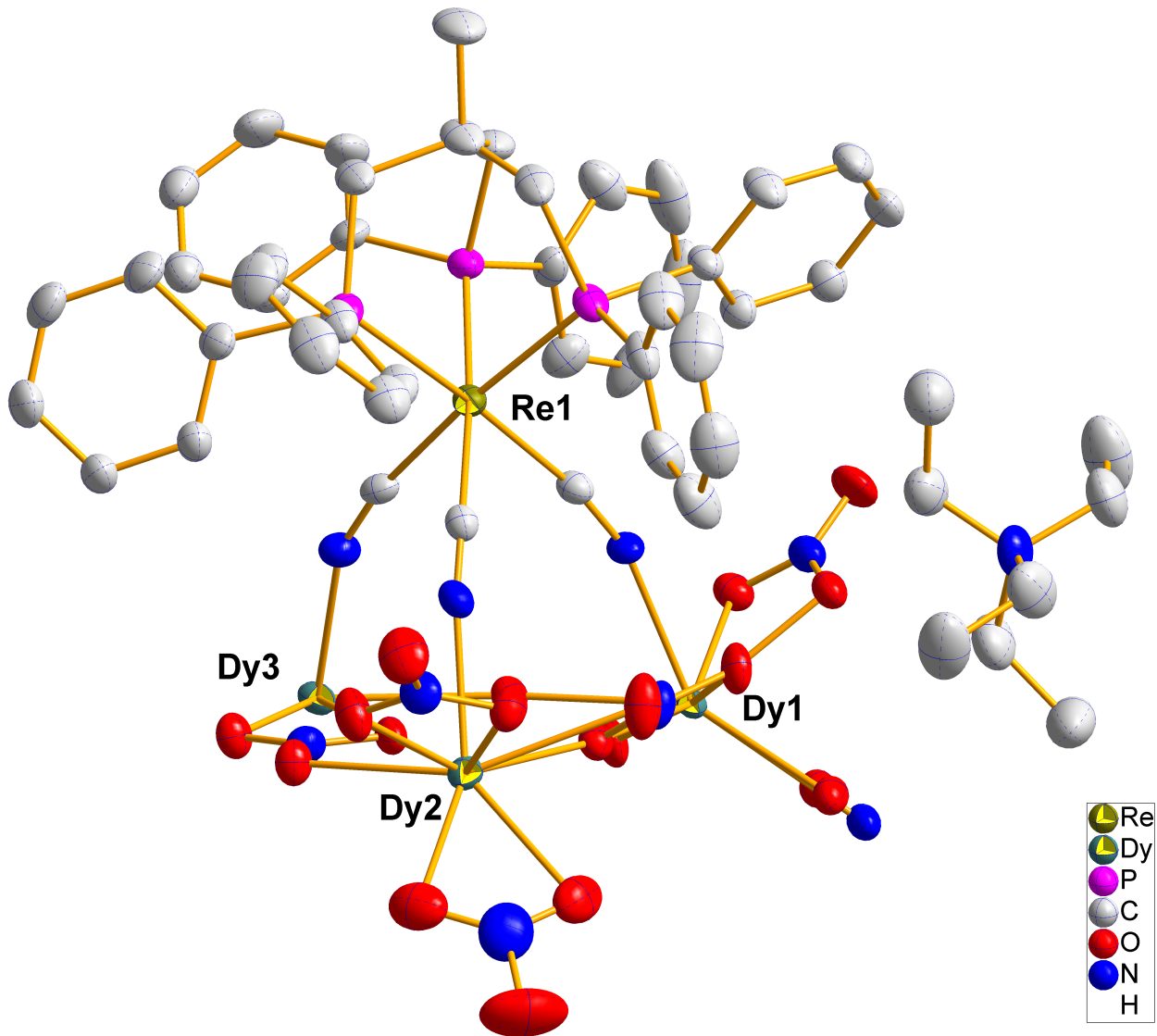
Compound	v(C≡N) cm ⁻¹		(NO ₃) cm ⁻¹		Ref	
[triphosRe(CN) ₃] ⁻	2060	2070	-	-	-	
1	2072	2090	1292	1089	834	This work
2	2086	2102	1297	1091	835	This work
3	2086	2103	1298	1091	836	This work



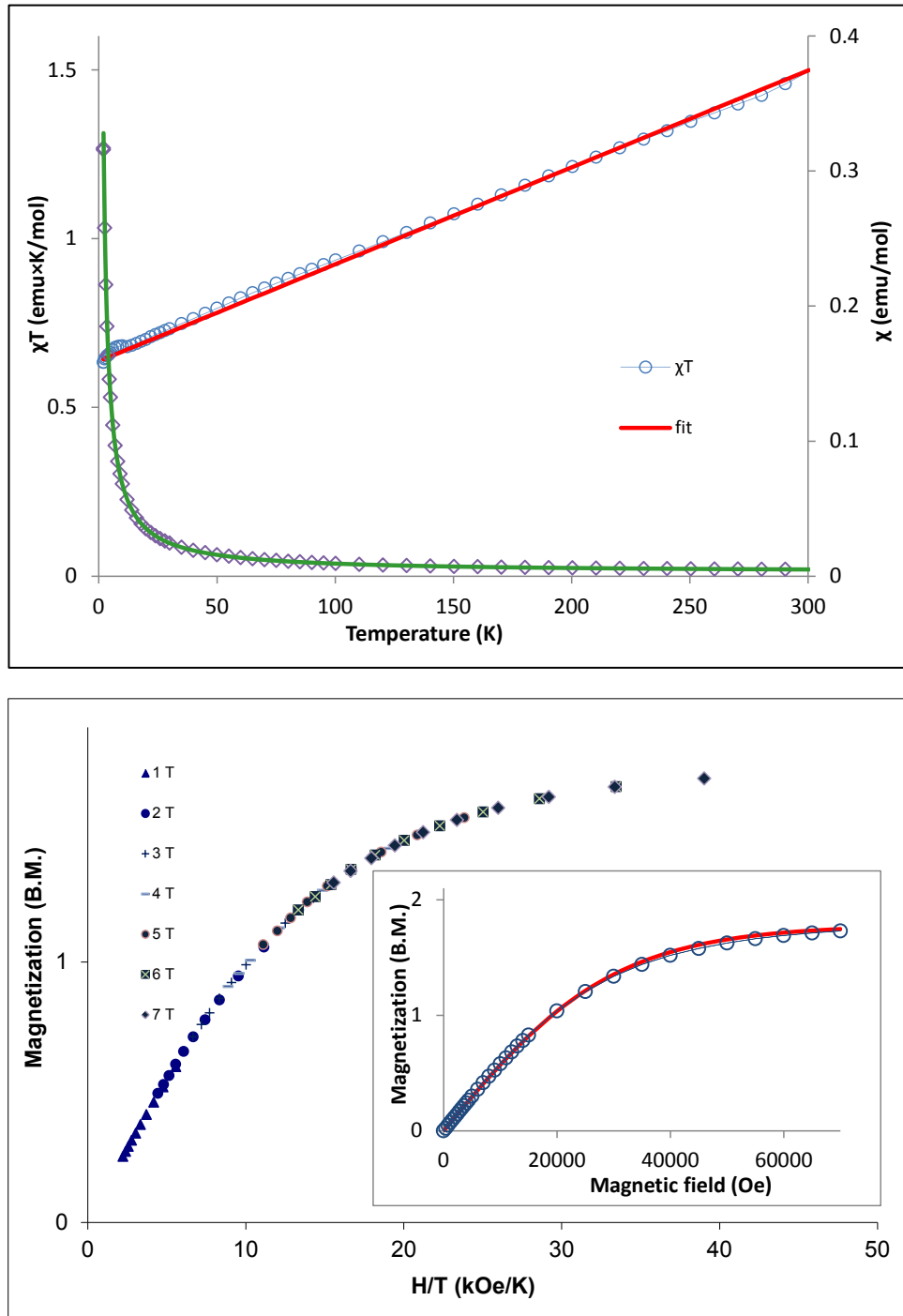
S 1. Distorted hexadecahedron polyhedron of La^{3+} center in **1** (top). Asymmetric unit of **1**. Thermal ellipsoids drawn at 30% probability. Hydrogen atoms omitted for the sake of clarity.



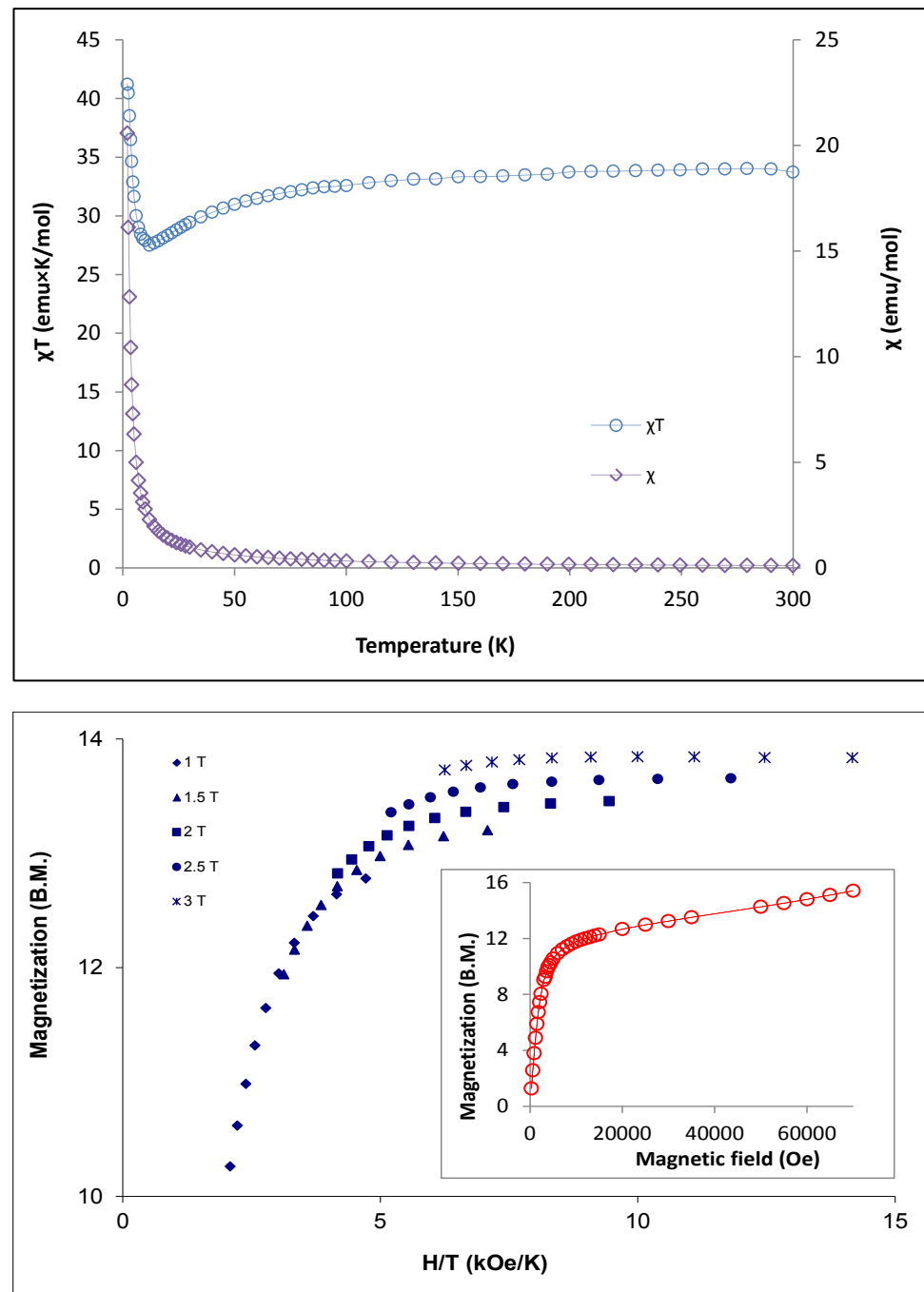
S 2. Asymmetric unit of **2**. Thermal ellipsoids drawn at 30% probability. Hydrogen atoms omitted for the sake of clarity.



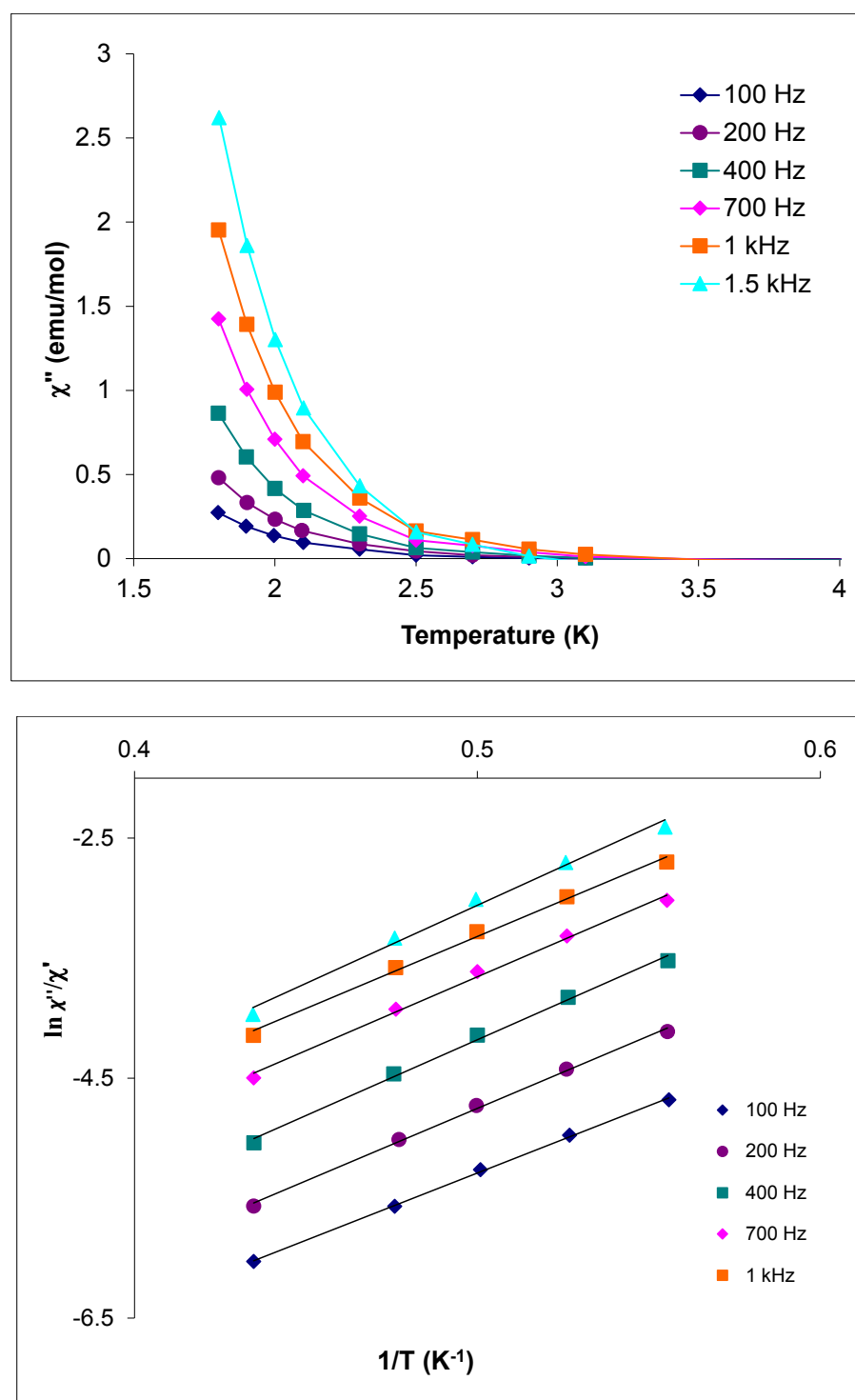
S 3. Asymmetric unit of **3**. Thermal ellipsoids drawn at 30% probability. Hydrogen atoms omitted for the sake of clarity.



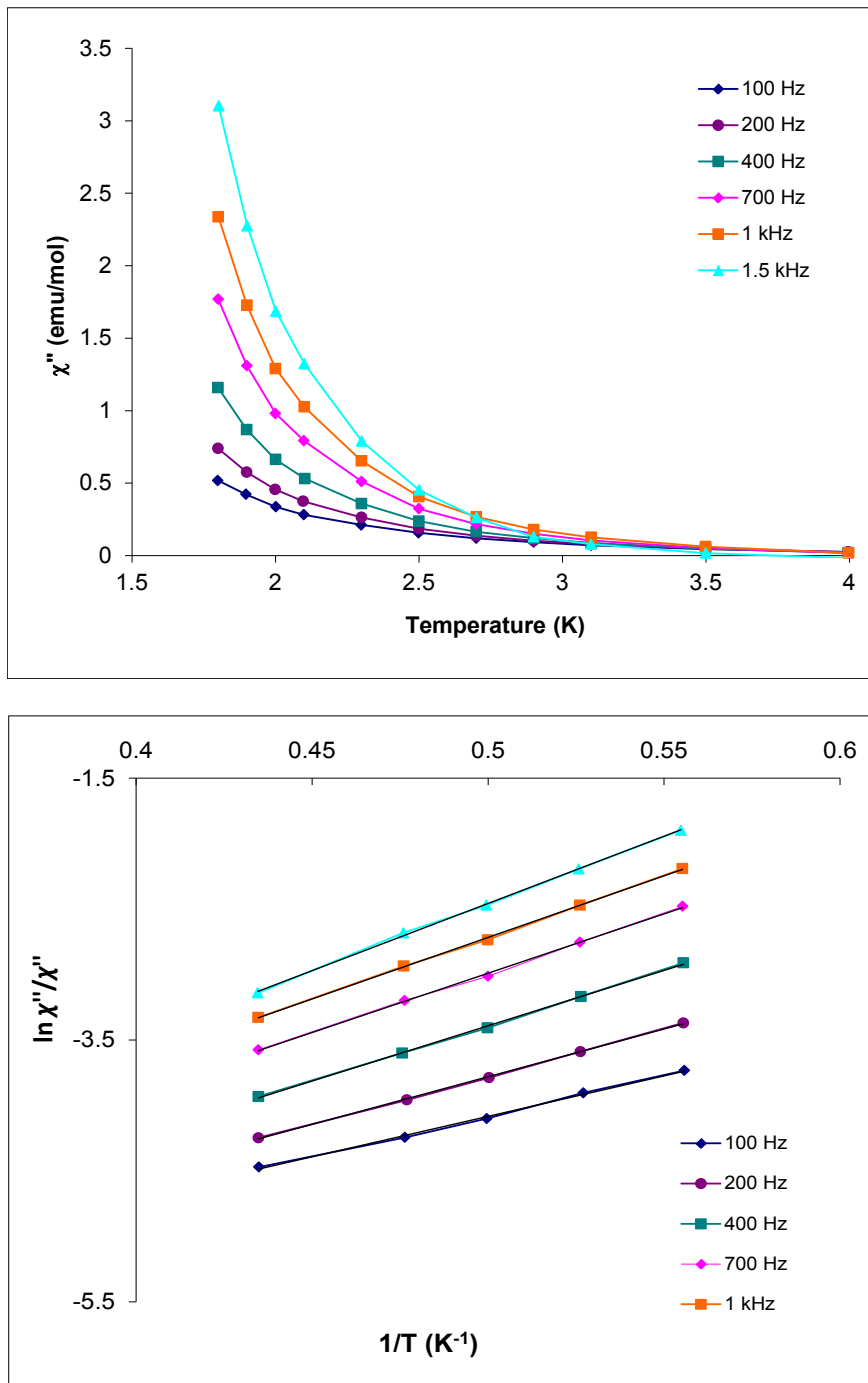
S 4. (a) Temperature dependence of χ (\diamond) and χT (\bullet) for **1**. Solid line corresponds to fit using PHI ($S=1/2$, $g = 1.88$ and $TIP = 2.49 \times 10^{-3}$). (b) Reduced magnetization data at different external fields. Inset: field dependent magnetization. The solid line corresponds to the Brillouin function ($S = 1/2$, $g_{avg} = 1.78$).



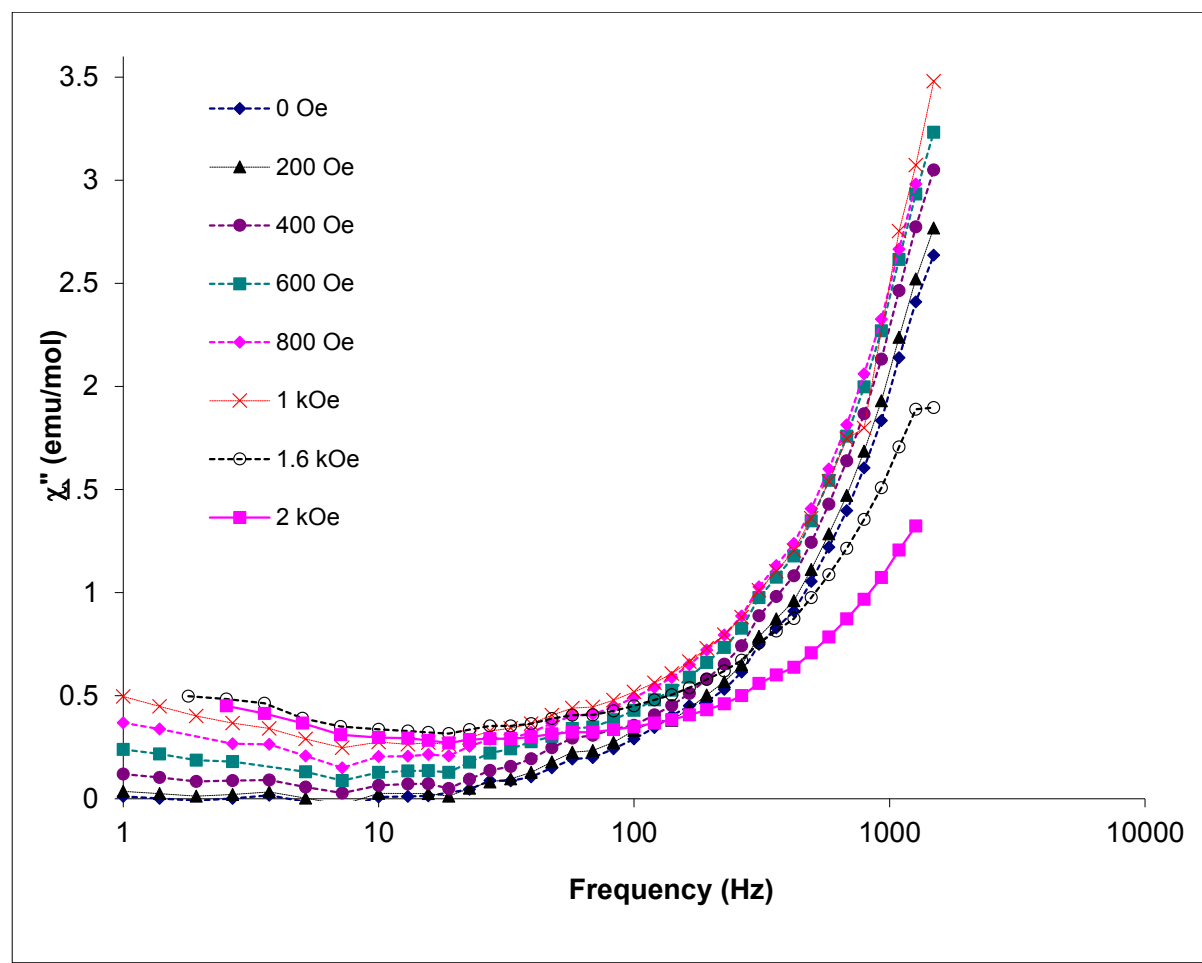
S 5. (a) Temperature dependence of χ (◊) and the χT product (○) for **2**. (b) reduced magnetization data at different external fields. Inset: field dependent magnetization for **2** (○).



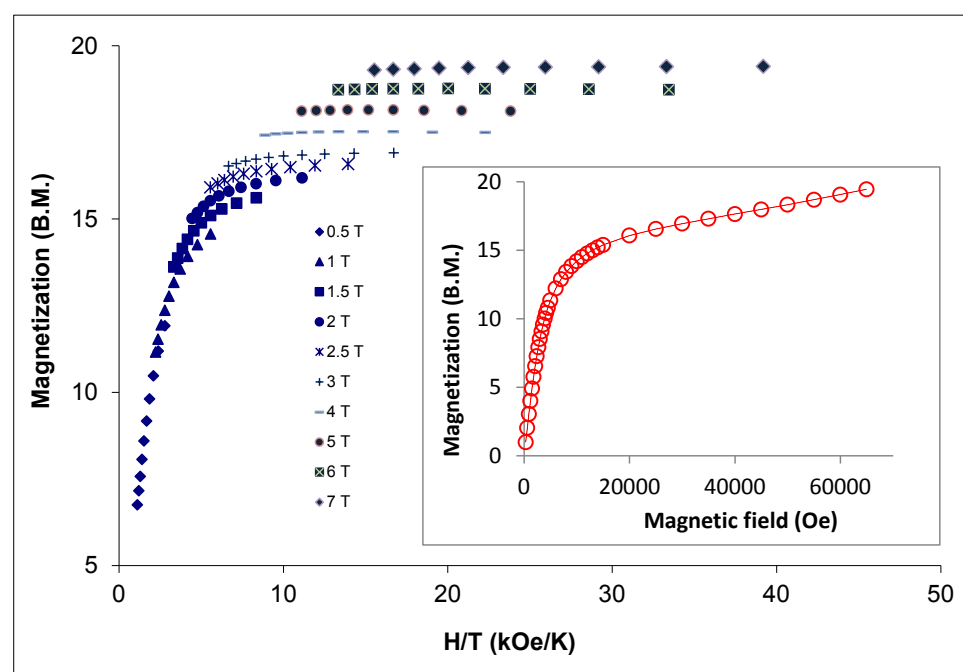
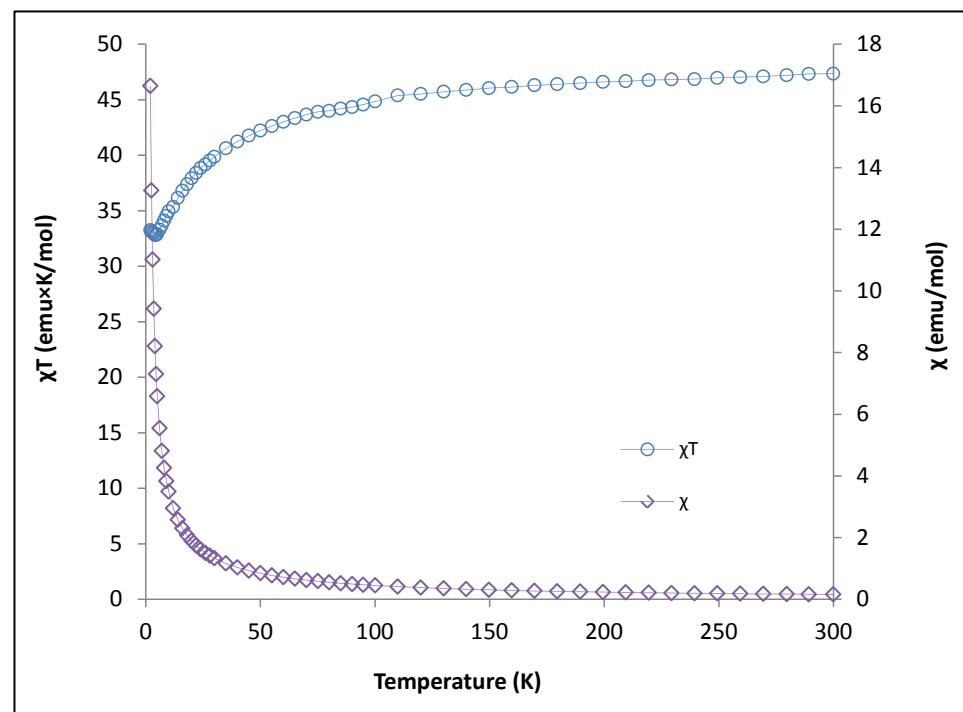
S 6. Temperature dependence of the out-of-phase AC susceptibility of **2** (top) and fit of the temperature dependence of the AC susceptibility data for **2** (bottom) under a zero applied DC field.



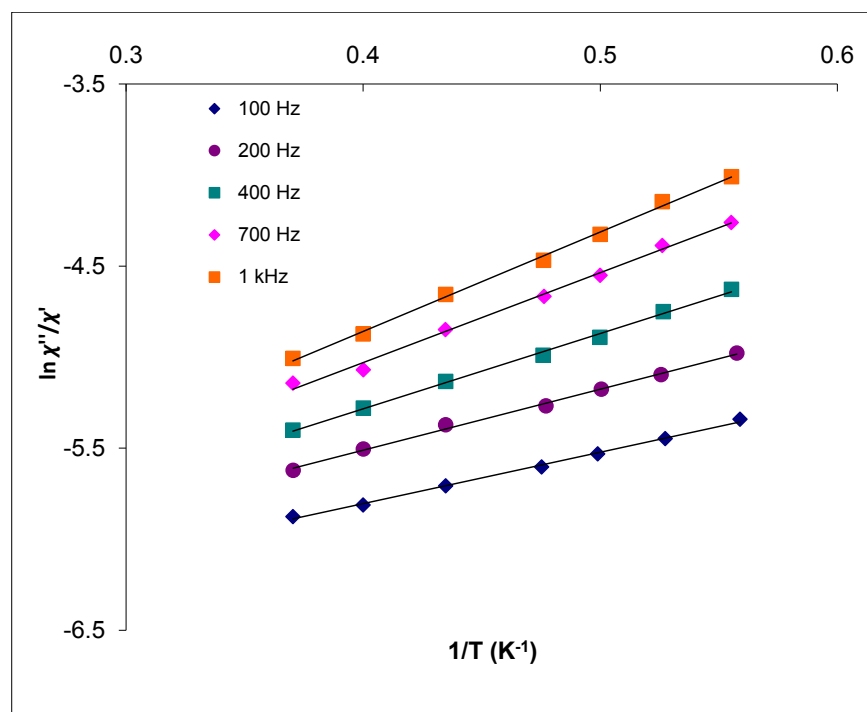
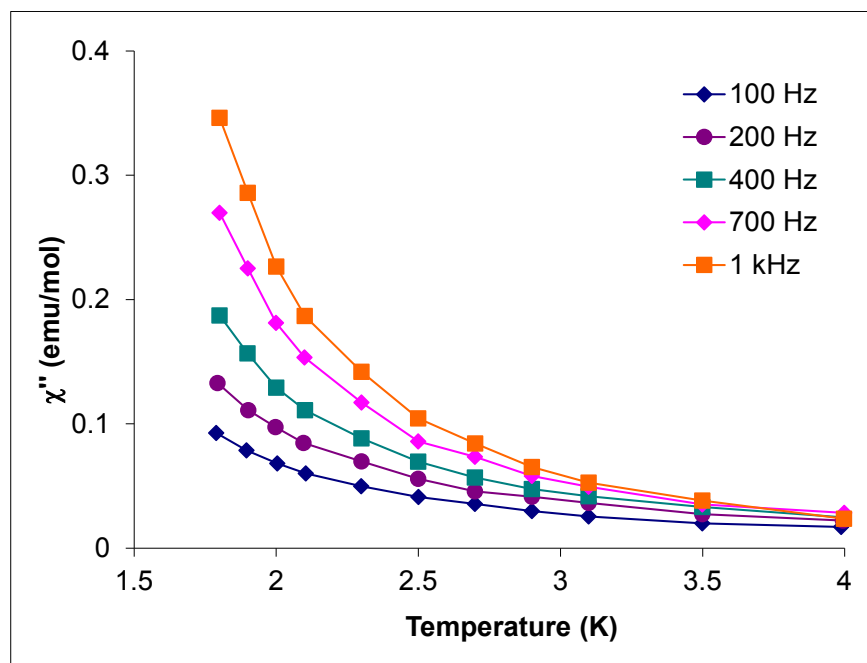
S 7. Temperature dependence of the out-of-phase AC susceptibility of **2** (top) and fit of the temperature dependence of the AC susceptibility of **2** (bottom) under a 1000 Oe DC applied field.



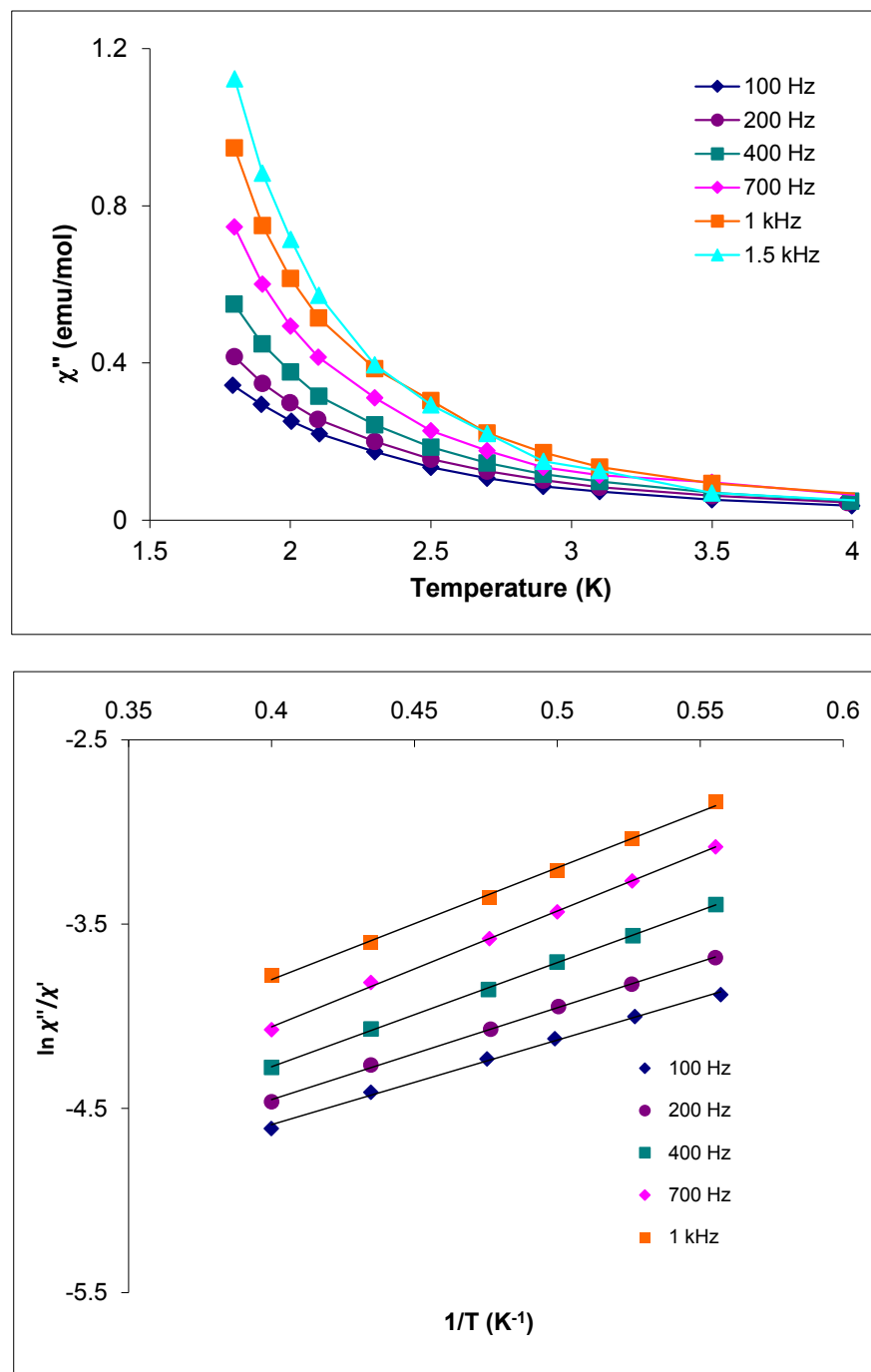
S 8. Field dependence of the AC data for **2**.



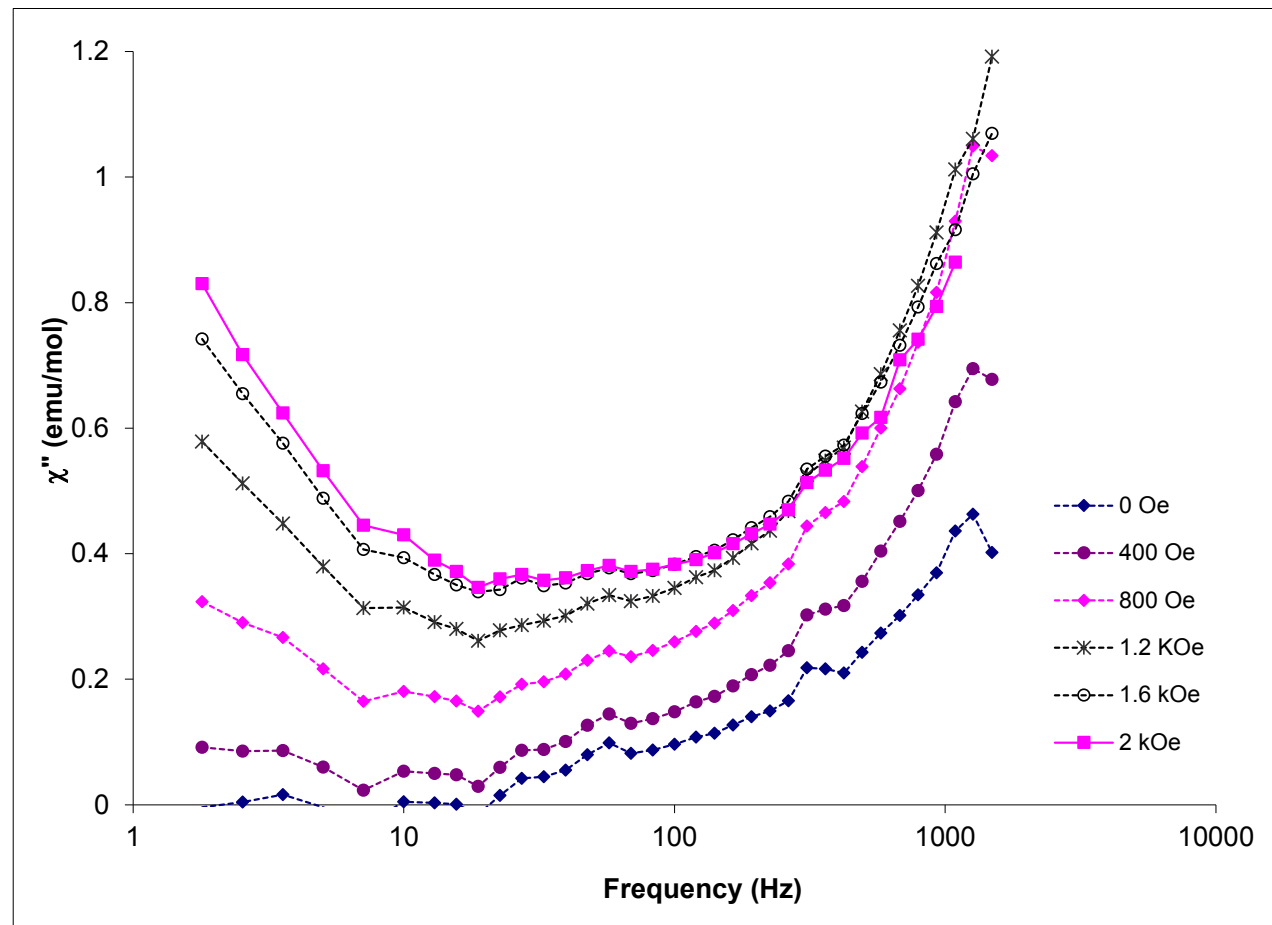
S 9. (a) Temperature dependence of χ (◊) and χT (○) for **3**. (b) reduced magnetization data at different external fields. Inset: field dependent magnetization for **3** (○).



S 10. Temperature dependence of the out-of-phase ac susceptibility of **3** (top), and fit of temperature dependence of ac susceptibility for **3** (bottom) under a zero DC applied field.



S 11. Temperature dependence of the out-of-phase AC susceptibility data of **3** (top) and fit of the temperature dependence of AC susceptibility data for **3** (bottom) under a 1000Oe DC applied field.



S 12. Field dependence AC data for 3.

1. E. J. Schelter, J. K. Bera, J. Bacsa, J. R. Galan-Mascaros and K. R. Dunbar, *Inorg. Chem.*, 2003, **42**, 4256-4258.
2. SMART and SAINT, 1996, Siemens Analytical X-ray Instruments Inc., Madison, WI.
3. G. M. Sheldrick, SADABS, 1996, University of Gottingen: Gottingen, Germany.
4. M. Sheldrick George, *Acta Crystallogr A*, 2008, **64**, 112-122.
5. L. J. Barbour, *J. Supramol. Chem.*, 2003, **1**, 189-191.